



OPEN Characterization of the natural fibers extracted from the aninga's stem and development of a unidirectional polymeric sheet

Jucelio Lima Lopes Junior^{1,3}✉, David Rodrigues Brabo¹, Everton Leandro Santos Amaral^{2,3}, André Wilson da Cruz Reis⁴, Cristine Bastos do Amarante³ & Carmen Gilda Barroso Tavares Dias¹

A unidirectional sheet was made with oriented fibers in an epoxy matrix. Natural fibers were extracted from the stem of *Montrichardia linifera* (Arruda) Schott., traditionally known as aninga, characterized and used to produce a unidirectional polymeric sheet. FTIR, XRD, SEM, TG, and DTG analyses were performed to characterize these cellulose fibers. Peaks observed at 1024 cm^{-1} , 1600 cm^{-1} , and 3328 cm^{-1} revealed the stretching vibration of the O–H bond, the stretching of the carbonyl in hemicellulose, and the vibration of aromatic rings, respectively. XRD analysis demonstrated a crystallinity index of 62.21%. Morphological analysis revealed the microstructural quality of the fiber surface, with grooves for mechanical anchoring, as well as its interior, which is composed of microfibrils. EDS analysis confirmed the presence of the main elements composing natural fibers, with carbon being the major component (70%). The thermal stability of aninga fibers was up to $450\text{ }^{\circ}\text{C}$ for the degradation of 50% of their initial mass. The mechanical properties of untreated aninga fibers showed a tensile strength of 332 MPa and an elastic modulus of 13.000 MPa. The unidirectional sheet had a tensile strength of 4.5 MPa and an elasticity modulus of 332.9 MPa. These outcomes ensured that aninga fiber is considered high-performance ($> 200\text{ MPa}$) and can be used for internal automobile components.

The study of natural fibers inside composite materials is an important matter to the industry because they have favorable mechanical properties and an ecologically sound nature¹. This interest is emergent among researchers in polymeric composites related to renewable resources. Finishing up cellulosic materials, such as fibers and particles, is lightweight, ecological, renewable, abundantly available, and biodegradable². The composites reinforced with natural fiber are excellent in strength-to-weight ratio, accessible cost, and environmental impact. Therefore, natural fibers offer significant advantages for commercial and engineering applications³. It is advisable to use natural fibers due to their eco-friendly nature⁴. For instance, tensile and flexural properties were excellent in a coconut fiber material with shell powder and vinyl ester, manufactured using the *hand lay-up* method⁵. A biocomposite based on polypropylene and waste from the plant species *Astrocaryum murumuru* was produced, and the results of the mechanical tests were competitive with other products made from different plant raw materials⁶. For those reasons, a sustainable and integrated design (structural and thermal) represents a significant field of research today regarding materials with components of natural origin⁷.

The plant species under study is the *Montrichardia linifera*, an aquatic macrophyte from the Araceae family, commonly known as “aninga”, vastly distributed throughout the Amazonian floodplain and equally found in different flooded ecosystems, such as igapós, igarapés, riversides, and water channels⁸. The use of this plant fiber is promising as it comes from a widespread and abundant plant species in the Amazon region, which ensures a renewable supply for its use as a raw material. Its prevalence is further favored by the heliophilic characteristics of the species, which exhibits a distinct affinity and preference for thriving under substantial exposure to sunlight, a defining feature of the Amazon region. This species is distributed in tropical regions; however, there is no record of occurrence in the Brazilian Pantanal. The “aninga” has a large ecological range, meaning it can be

¹ Postgraduate Program in Mechanical Engineering, Federal University of Pará, Belém, Pará, Brazil. ² Faculty of Mechanical Engineering, Institute of Higher Studies of the Amazon, Belém, Pará, Brazil. ³ Coordination of Earth Sciences and Ecology, Museu Paraense Emílio Goeldi, Belém, Pará, Brazil. ⁴ Postgraduate Program in Amazon Natural Resources Engineering, Federal University of Pará, Belém, Pará, Brazil. ✉ email: juceliolopesjr@gmail.com

found from emergent to terrestrial areas in water-saturated soil. In most cases, aninga forms extensive forests, popularly known as “aningais”, which are formed through the sprouting of underground submerged stems, resulting in clonal populations of the plant⁹, each reaching approximately 3 to 6 m in height, with variable stem thickness. The size of the leaf structure averages around 40 cm in width. This species is herbaceous, reaching a height of 4–6 m. It has an aerial stem with evident nodes, internodes, and a widened base. The infructescence of *Montrichardia linifera* is of green to yellowish-green color as a whole; it has no aroma, and it is similar to pineapple externally. The fruits (fruitlets) are characterized by a conical shape with a pale-yellow color on the inside, releasing a persistent and unpleasant astringent aroma⁸. In the Amazon region, the aninga develops with a maximum production of alpha-cellulose, which can be higher than the amounts found in the plant as observed in other regions of Brazil. The plant is part of the food chain of some animal species, such as fish and turtles⁸, and aquatic mammals like the manatee⁹. However, studies have shown that the leaves and the infructescence, which are the most consumed parts of the plant, have shallow protein values for the animals that feed on them. Another obstacle is related to the consumption of this plant *in nature*, as it contains levels of manganese in its composition that are considered toxic, even for large animals like bulls and buffalos⁸. Tests conducted on this plant species have demonstrated the quality of the fibrous material present in the stem region, allowing the use and application of the fiber in various areas of knowledge. The proven technological potential of the species is attributed to the considerable presence of fibrous material in the plant, especially in the interior of the stem, as well as its high mechanical resistance of 8.206,20 gf/mm²¹⁰. The *Montrichardia linifera* fiber is extracted from the stem and it is classified as bast fiber. Therefore, they are among the longest fibers studied, with fibrous bundles extracted up to 2.50 m long. In addition to their considerable length, they exhibit high tensile strength, approximately two times the strength of coconut fiber [Number]. The aninga fibers have a light coloration, which implies their chemical composition, is mostly cellulose-based. It is important to emphasize that in the case of fibers derived from natural resources, a higher amount of cellulose and low lignin content result in greater tensile strength¹¹. However, little is known about this fibrous material and its potential uses, and therefore, it is necessary to continue such studies. The fibers of the species are long and light in color, present within the stem of the plant. Their arrangement inside extends from the endodermis of the stem bark to the core, amid other tissues that make up the internal structure. Due to it being a fibrous plant, the extraction of its assets results in a considerable quantity of fibers at the end of the process.

The technological use of long fibers such as those from *Montrichardia linifera* has already been reported in the literature, similar to the fibers from banana stems, where microstructural and elemental analyses confirmed that laminates with fibers from the species strengthened a composite material due to the continuity of the fiber, resulting in less damage to the structures of the fibers¹². The aim of this research was the characterization of aninga fiber and its application in a composite. The results presented in this article are part of a patent application in progress in Brazil, related to the described invention.

Materials and methods

The collection of the species *Montrichardia linifera* does not require specific authorization according to current Brazilian legislation, as this species is not listed as endangered and was not collected in a Protected Area. According to Article 8 of Law N° 11,428/2006, which regulates the use and protection of native vegetation, the collection of non-endangered species outside protected areas is exempt from specific authorization. Furthermore, this research has been duly registered in the National System for the Management of Genetic Heritage and Associated Traditional Knowledge (SISGEN), under registration number A91B68B, affiliated with the Museu Paraense Emílio Goeldi. The areas for collecting the plant samples were the Research Campus of MPEG and the Mangal das Garças Ecological Park. The plant material and stem samples were collected along the banks of the river in the Guajará Bay region, near the Mangal das Garças Ecological Park, Belém, Pará, Brazil (1°27'52.0"S 48°30'23.1"W). The park spans an area of approximately 40,000 m² and features floodplain forests with over three hundred species of native trees. The samples were taken to the laboratory and cleaned with running water to remove impurities. Batista R.J.R identified the plant and the herbarium specimen was deposited at the João Murça Pires Herbarium, at the Emílio Goeldi Museum in Pará, under the registration number MG 216,695. The fibers were extracted using the dew retting method, in which biological material decomposes at room temperature of 26 °C. After that, the fibers were extracted through mechanical manual extraction after 14 days¹³. Aspects related to the attack of organisms on the fiber structure were also considered, given that biological attacks can lead to the degradation of the fiber structure over time (Fig. 1).

SEM images were acquired using a Tescan Mira3 microscope equipped with a FEG-type electron gun, and the images were captured via secondary electron detection at 5 kV with working distances of 10–15 mm, FTIR was made with the equipment Cary 360 (Agilent, Santa Clara, CA, USA) with a zinc selenide (ZnSe) crystal and an ART module., XDR machine was (Cu Ka 35 kV and 30 mA), model Malvern Panalytical, 2θ scans ranging from 10° to 40° at a scan rate of 0.01°/min, with approximately 5 g of fiber powder used for each analysis. The data obtained was processed using PeakFit V4.12 and OriginPro8 software to create graphs, with X'Pert HighScore Plus to determine crystallographic diffraction planes and patterns. The epoxy resin was Epoxy system DGEBA composed of REX 135 resin and Hex 135 SLOW hardener, mixed in a mass ratio of 100 parts resin to 33 parts hardener, then the sheet was formed using the wet filament winding process¹⁴, the filament winding equipment is a custom-made device created in the Eco Composites Laboratory, where the fibers were oriented at a 90° angle. The fibers and the laminates were tested for tensile strength¹⁵. The fibers and the sheet tensile strength test were made at a Universal Machine EMIC, where 10 specimens from the sheet were pulled at a test speed of 50 mm/s, with an initial distance between claws of 70 mm.



Fig. 1. Aninga fiber extraction: (a) Aninga plant; (b) Stem on maceration process; (c) Fiber manual extraction; (d) Unidirectional sheet.

Results and discussion

Fourier transform infrared spectroscopy (FTIR) analysis

The aninga plant fiber exhibited transmittance bands at 3328 cm^{-1} , 1600 cm^{-1} , and 1021 cm^{-1} as the main functional groups in its composition. The FTIR spectrum of *Montrichardia linifera* fibers with the exact band locations, followed by the assignments of functional groups in the natural fiber was shown in the responses of the bands between $580\text{ e }4080\text{ cm}^{-1}$ were used to identify cellulose, hemicellulose, and lignin components in the fiber (Fig. 2).

The plant fiber of the *Cyperus platystylis* species had its main incidence at 3402 cm^{-1} corresponding to the stretching of the O–H cellulose bond¹¹. The strong and broadband at 3332 cm^{-1} in fibers of the *Furcraea foetida* species was associated with the stretching vibration of the hydrogen bond O–H (alcoholic group) of the hydroxyl group in the molecules of α -cellulose.

The peaks at 3328 cm^{-1} ; 3334 cm^{-1} , 3341 cm^{-1} , and 3363 cm^{-1} correspond to the stretching vibration of the O–H bond^{16–18} and the presence of α -cellulose^{19,20}.

The point at 1632 cm^{-1} indicates the stretching of the C=C bond, representing the lignin constituents in the *Grewia Flavescens* fiber^{19,20}. The peak at 1606 cm^{-1} is attributed to the stretching of acetyl groups in lignin²⁰. The intensity of the peak observed at 1649 cm^{-1} corresponds to the vibrational bending of the OH–OH groups, which confirms the presence of α -cellulose in the samples. The authors emphasized that with the peaks found at 1629 cm^{-1} and 1050 cm^{-1} , cellulose, hemicellulose, and lignin were present in the *Manau rattan* fiber²¹.

The point at 1036 cm^{-1} corresponds to the deformation plane of the aromatic ring of lignin²². The characteristic peaks at around 1026.13 cm^{-1} correspond to C–O and O–H stretching vibration, including cellulose polysaccharides¹⁷. The point at 1044 cm^{-1} represents the stretching of the C–O bond of the acetyl group in lignin¹⁹. The ramie fiber showed peaks at 1032 cm^{-1} (stretching of the C–O–C bond)¹⁸. Bands between 1155 and 1020 cm^{-1} are typically associated with the stretching vibration of C–O and O–H, belonging to the polysaccharide in cellulose. Thus, the glycosidic bonds indicate cellulose because these bonds link the anomeric carbon atoms of the saccharides to form polysaccharides/polycarbohydrates²⁰.

Based on the analyses above, the FTIR results on the aninga fibers confirmed the presence of functional groups found in the main components of natural fibers, such as cellulose, hemicellulose, and lignin.

X-ray diffraction (XRD) analysis of the aninga fiber

It was observed peaks of intensity between 15° e 25° (2θ) on the x-ray diffraction (XRD) spectrum of the powder from the aninga fiber, the main peak was at 24.7° which corresponds to the diffraction of the crystalline cellulose cell wall, and the remainder corresponds to the amorphous structure, which characterizes vegetable-derived structures. Observing the X-ray diffraction (XRD) spectrum on the fibers of the species *Montrichardia linifera* is possible (Fig. 3).

The first peak at 15° in the (1 1 0) plane demonstrates the presence of the amorphous material in the fiber²³, a structural component of the fiber bundles. The second peak at 25° indicates the presence of the crystalline cellulose structure in microfibrils on the fiber surface²⁴. It is possible to notice that the intensities of the peaks are well-defined, clearly indicating the existence of crystallinity. Cellulose exhibits a crystalline structure given the hydrogen bonds that this material is capable of forming within its structure, as well as due to the Van der Waals forces existing between the molecules.

The peak near 16.00° corresponds to the amorphous material such as cellulose, hemicellulose, and lignin^{20,25}.

The points near 22.00° may be related to the crystalline material, which can be attributed to cellulose type IV in lignocellulosic fibers²¹. The samples exhibited peaks related to characteristic crystalline planes of lignocellulosic materials at 22° , corresponding to the reflection coordinate plane (0 0 2), with peaks at (16°) (1 1 0), (16.5°), (22°) (2 0 0), and (22.5°), representing cellulose-I^{26–30}.

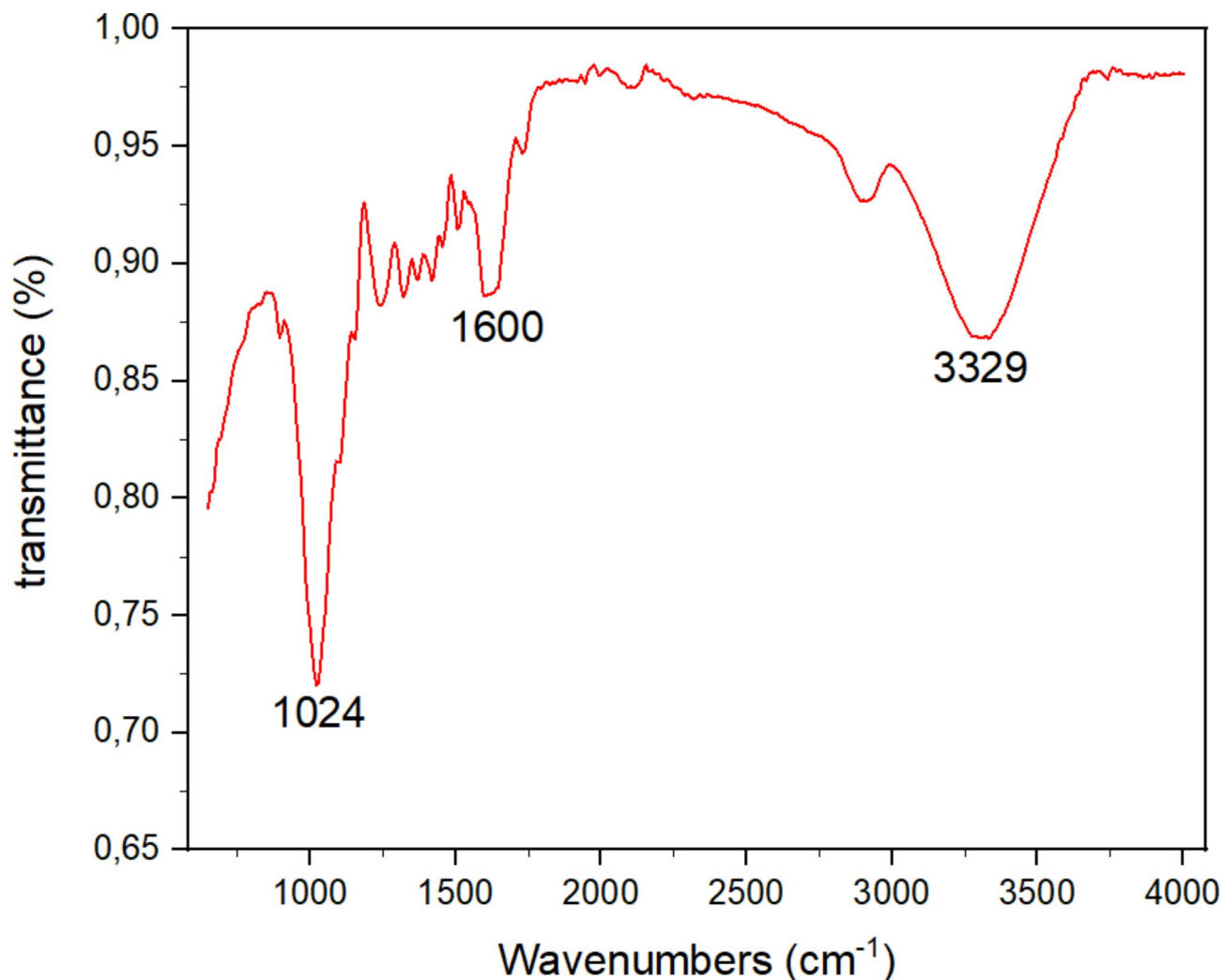


Fig. 2. FTIR analysis of aninga cellulosic fiber.

These peaks are similar to those reported in the literature for other plant fibers, which mainly exhibit a cellulosic structure, where the spectrum shows a strong, broad diffraction peak around 22° , consistent with the diffraction patterns (0 0 2) of carbon³¹.

The chemical composition varies among all natural fibers. For instance, cellulose is more abundant in sisal, hemicellulose is more present in bamboo, and lignin is in piassava fibers. This demonstrates the compositional similarity of aninga fiber to sisal fibers due to the high peak in the crystalline region of cellulose.

In the results of the investigation of the crystallinity index (X_c), the aninga fiber exhibited a crystallinity index of 62.21%, such index shows highly crystalline cellulose similar to fibers from the species *Corypha taliera*¹⁷, which indicates a high cellulose content in the fibers, with the high-intensity crystalline peak at $24,7^\circ$ (2θ). The fibers of *Montrichardia linifera* are mainly composed of cellulose, whose crystalline nature provides a rigid structure. This index was higher than those found in other species, such as *E. indica* (45%), *C. seloana* (22%), *P. orientale* (33.5%), *S. ehrenbergii* (52.27%), and similar to that found in the *Typha angustata* grass species of 65.16%^{23,32–37}.

SEM-EDS of the aninga fiber

The study of the morphology of natural fibers is critical, as it confirms the usability of fibers as suitable reinforcement in composites manufacturing. Observation of the raw fiber's surface reveals the typical cellulose structure, organized into aggregated microfibrils with submicrometric diameter, forming fibrous structures with cylindrical cross-sections, called bundles³⁸. On the surface of *Montrichardia linifera*, it was possible to observe the presence of pores, which according to the literature increases the roughness of the fiber surface³⁶. This is a desirable phenomenon for the fiber to achieve greater bonding with the polymer. Similar to *Juncus effusus* fibers, where it was reported that the fiber surface contained rough cavities with small voids³⁹.

The vascular tissue of *Montrichardia linifera* is mainly formed by tracheids, which are vascular structures of plants, as well as the abundant presence of fibers. The longitudinal microstructural view of the stem fiber of *Montrichardia linifera* exhibits a structured arrangement with a rough surface, similar to what was observed in

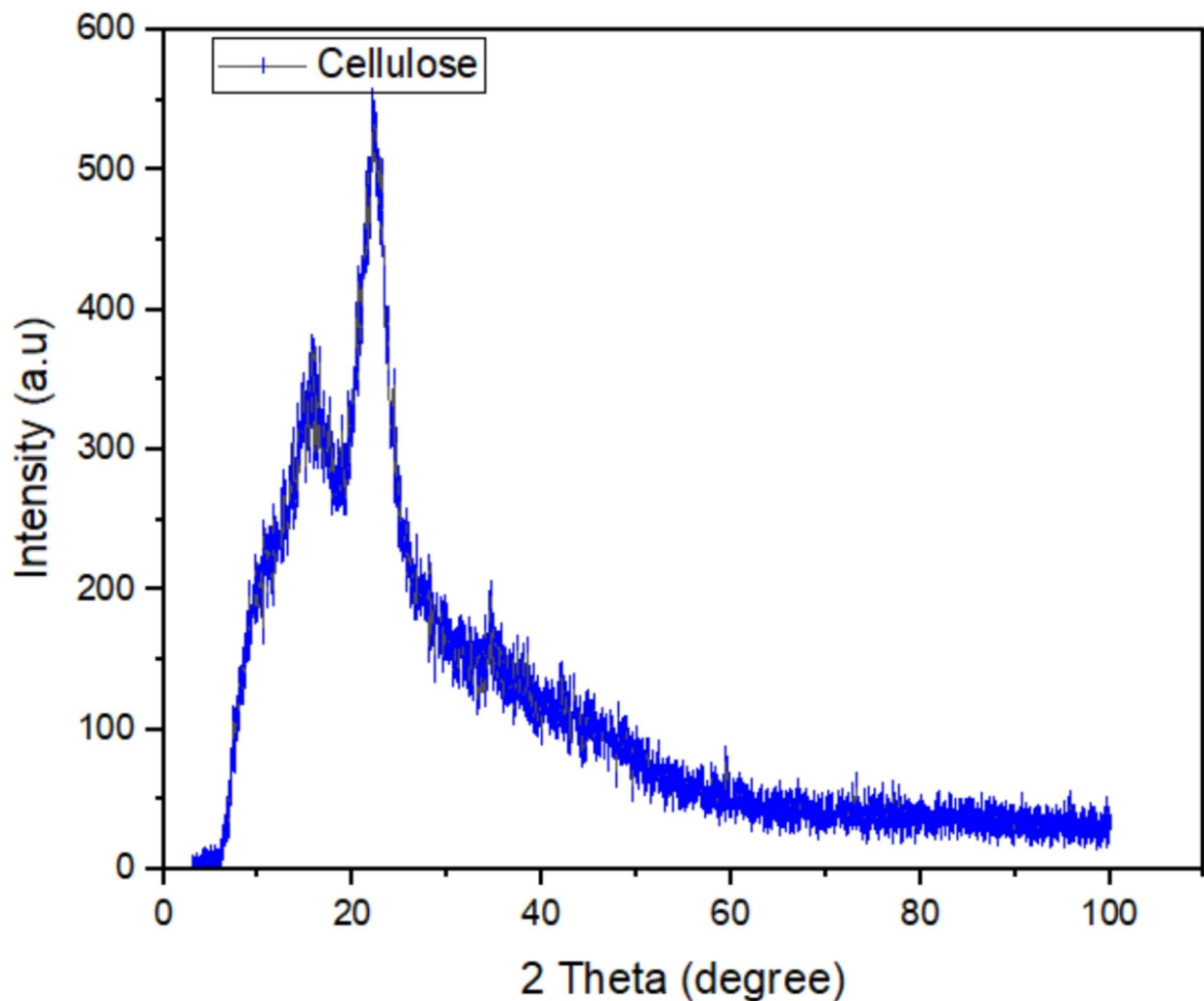


Fig. 3. X-ray diffraction (XRD) analysis of the aninga fiber.

the fiber of *Grewia damine*⁴⁰, emphasizing that the fiber is suitable for the fabrication of new composites with good mechanical characteristics (Fig. 4).

The longitudinal microstructural view of the stem fiber of *Montrichardia linifera* exhibits a structured arrangement with a rough surface, similar to what was observed in the fiber of *Grewia damine*, where it was emphasized that the fiber is suitable for manufacturing new composites with good mechanical properties⁴⁰.

The fibers of *Montrichardia linifera* are composed of microfibrils that are united in a single bundle forming the structure of the fibers, which are similar to the fibers of *Grewia Flavescens*, where it was observed that the fibril is linked to the fiber by pectin, as well as by non-cellulosic compounds²⁷. The *Manau rattan* fibers consist of aligned elementary fibers united by non-cellulosic components. Additionally, the morphology of the *Manau rattan* surface is rough, which favors the bonding of the fiber and the polymeric matrix in composites⁴¹.

Scanning Electron Microscopy (SEM) images of the fibers have shown that the material does not contain silicates in its composition; instead, it is rich in cellulose. The vascular tissue of *Montrichardia linifera* is primarily formed by tracheids and fibers.

It was also possible to notice that the surface of the fiber bundles has grooves in a honeycomb-like structure, which is favorable for mechanical anchoring in association with polymeric resins. This is similar to the fiber of *Cyperus compactus*, which has matrices of regularly arranged cells in a square shape across the entire fiber surface³⁰.

The surface roughness contributes to an increased contact area to ensure better adhesion of the fiber to the matrix in both composite manufacturing and application⁴², as a smoother fiber surface hinders the interaction between them, reducing the bond between the fiber and the matrix⁴³. The honeycomb-like surface morphology also enhances bonding strength when used as reinforcement in the manufacturing of composites⁴⁴.

The SEM images of the sheet reveal strong adhesion between the fibers and the epoxy matrix, as evidenced by the fact that the materials at the cracking point fractured together. These images illustrate different types of interactions between the materials: there are instances of simultaneous cracking, as well as areas where the pull-

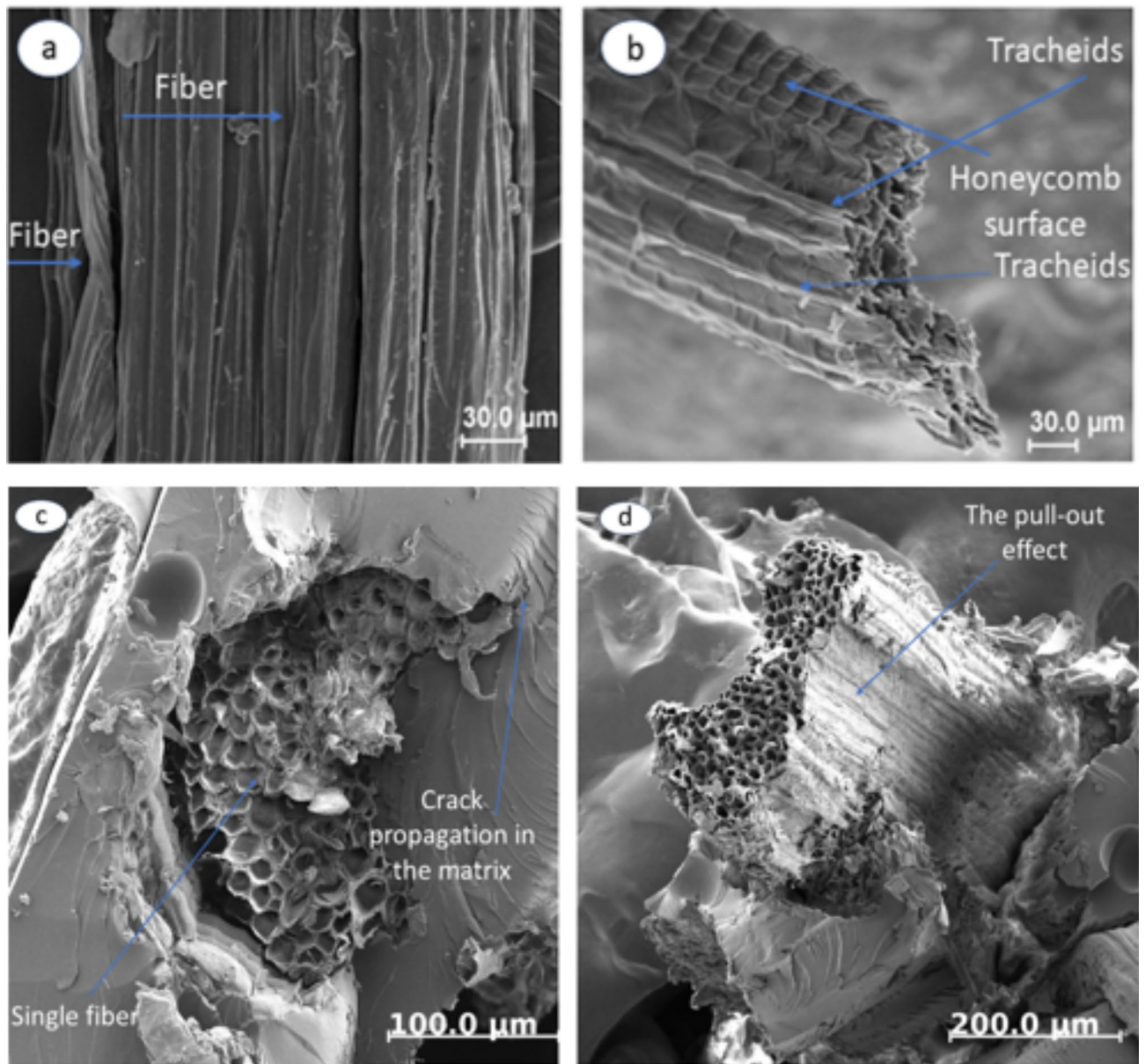


Fig. 4. Aninga's single fiber (a) longitudinal view and (b) cross-sectional view of the fiber (c) cross-sectional view of a test specimen subjected to tension (d) The pull-out effect of a single fiber inside the matrix.

out effect was observed in individual fibers within the matrix. However, the majority of the material fractured without evidence of pull-out.

Figure 5 presents the microscopic image of the analyzed point on the surface of the fiber of *Montrichardia linifera*.

The fibers of *Montrichardia linifera* exhibited carbon (71.26%) and oxygen (14.92%) as the major elemental components. Cellulosic fibers typically contain carbon and oxygen as dominant elements⁴⁵.

The higher amounts of carbon and oxygen elements ensured that the surface of the fiber of *Furcraea foetida* contained a lower quantity of lignin content⁴⁶, resulting in fewer amorphous constituents on the surface, which could potentially enhance bonding properties with polymeric materials. Similar proportions of compounds were found on the surface of *Montrichardia linifera* fibers.

Chemical elements such as carbon, calcium, and oxygen are some of the predominant components present on the surface of untreated fibers. Among these chemical elements, carbon was found to be a primary component. These elements were also found in the fibers of *Agave Lechuguilla*⁴⁷.

Results from EDS analysis confirm the presence of a high carbon content in natural fibers of pineapple, kenaf, and hemp, except for flax. The authors further emphasized that the chemical compounds revealed by EDS show the dominance of cellulose content over other substrates in kenaf fibers, which exhibited a composition of

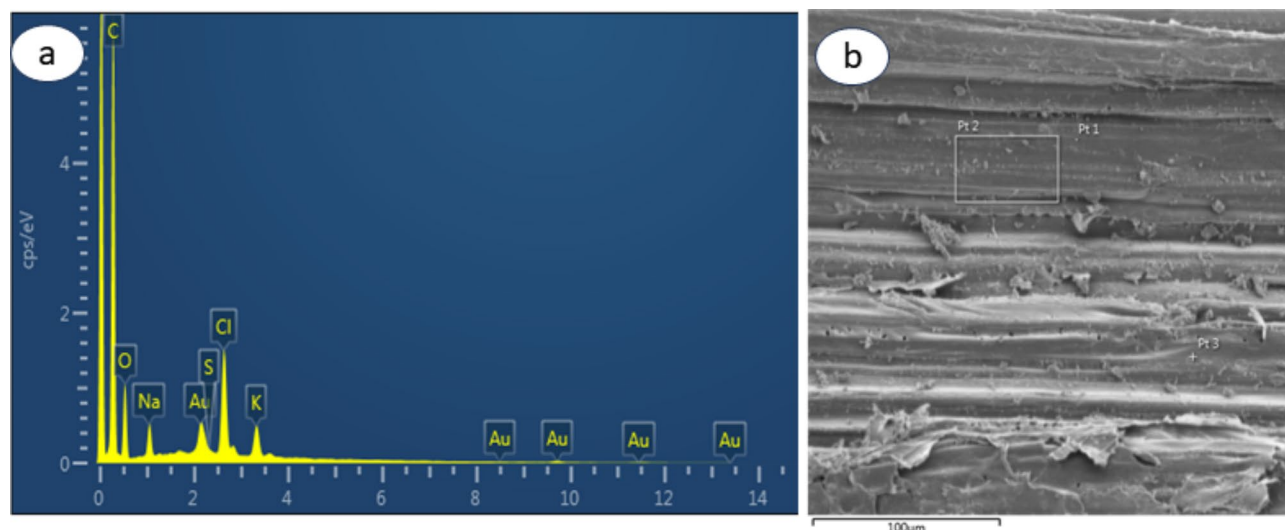


Fig. 5. EDS of the aninga fiber (a) elemental components (b) measure point.

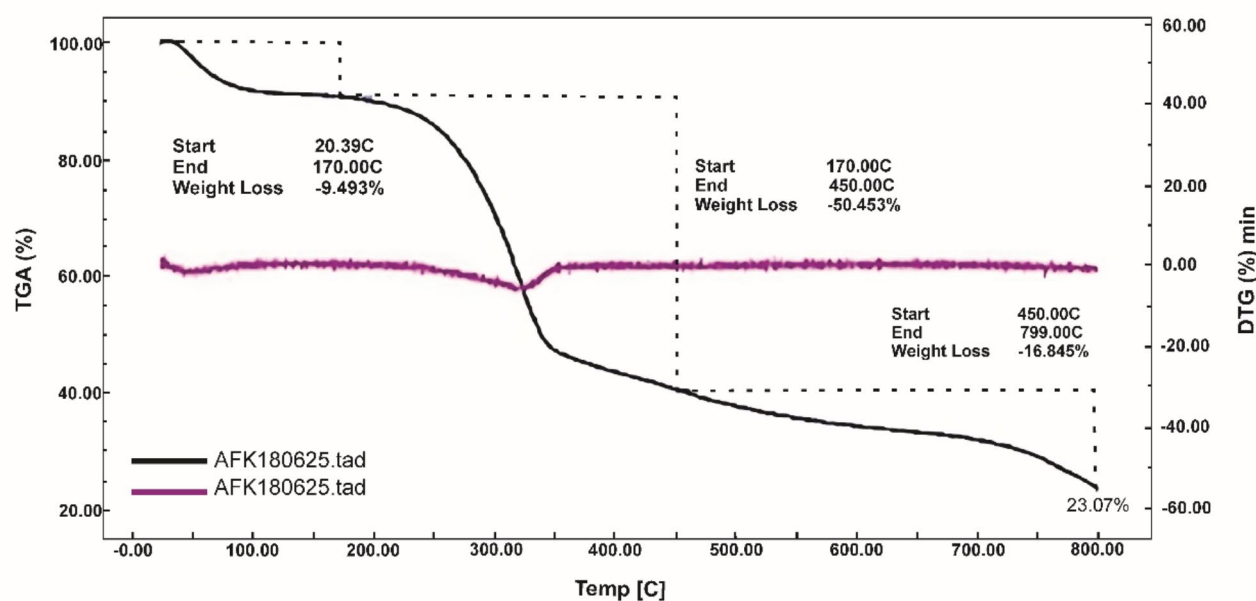


Fig. 6. TGA and DTG of the fiber.

54.36% carbon⁴⁸. The elemental composition in the bark of the *Holoptelea integrifolia* tree was C 85.59% and O 14.41%^{49,50}.

Thermal stability of the aninga fibers

The thermogravimetric analysis (TGA and DTG) curves of *Montrichardia linifera* fibers show the variation in the mass loss for the sample of the species as a function of temperature elevation. Mass losses related to the degradation process of the aninga fiber can be observed, especially the pyrolysis of its main constituents such as hemicellulose, cellulose, and lignin (Fig. 6).

The initial mass loss in the aninga sample was observed in the range of 20 °C to 170 °C, with a mass loss of 9.59% in this first peak. This variation in this temperature range can be attributed to moisture loss in the sample. Mass losses of approximately 6% below 200 °C have been found in samples of pineapple, kenaf, flax, and hemp fibers⁴⁸. The mass loss in the range from 35 °C to 91.9 °C is attributed to the evaporation of moisture from the new species of plant fiber³⁰. A mass loss result reported at a temperature of 89 °C was associated with the removal of moisture and wax⁴⁴. Cellulose biomass typically experiences mass loss around 100 °C due to the loss of moisture present in it^{49,50}. The mass loss in this temperature range for jackfruit fibers was reported as 6%. According to the authors, the initial weight loss occurs due to the evaporation of moisture on the fiber surface at

around 100 °C. This degradation pattern indicates that the fiber is rich in cellulose content and high crystalline structures⁴². Degradation at temperatures below 150 °C is primarily attributed to moisture loss in the fibers⁵¹.

The main peak of thermal degradation temperature between 200 °C to 400 °C is the temperature at which the mass loss rate due to thermal decomposition reaches its maximum value⁵². In the case of *Montrichardia linifera* fibers, this loss rate was 50.46%. The major mass loss event occurring between 300 and 400 °C is associated with the degradation of the primary compounds (cellulose, hemicellulose, and lignin) of the cellulose^{49,50}. The temperature range of 200 to 435 °C, where the highest degradation (> 60%) occurred in the plant fibers of *Grewia Optiva*, is the primary temperature range for processing some of the thermoplastics⁵³. In the second range of thermal degradation, there is a decrease in chemical constituents in the fiber sample^{44,54}. The peak maximum degradation occurs at 358 °C, primarily due to the degradation nature of α -cellulose (50% mass variation, 228–358 °C)⁴², given that cellulose-rich and highly crystalline structures increase degradation temperatures^{55,30}. The study that evaluated the thermal stability of açai fibers described the degradation processes of cellulose, hemicellulose, lignin, and pectin, among other constituent materials of plants in general.

The next stage (after 358 °C) is mainly involved in the decomposition of cellulose and lignin. Similar degradation behaviors have been reported in various cellulose-based natural fibers^{44,56,57}. The major mass loss event for cellulose cryogel occurred between 300 and 400 °C, corresponding to the degradation of the main compounds, such as cellulose, hemicellulose, and lignin^{49,50}.

The *Montrichardia linifera* species endured temperatures in the range of 400 °C, retaining 50% of its mass. Furthermore, its mass is composed of 23.07% mineral components that do not undergo combustion at a temperature of 800 °C, demonstrating a high ash (mineral) content and a low amount of organic matter.

Mechanical properties of the aninga fiber

The tensile test with the single fiber of *Montrichardia linifera* obtained the main characteristics of this fiber that are relevant for mechanical analyses. The aninga fiber presented a failure stress value of 308,3 MPa and an elastic modulus of 13.873,25 MPa. The tensile strength value falls within the mechanical tensile strength range of the main natural fibers used in composites (Table 1), and the fiber's elastic modulus value was highly elevated, indicating that the elastic deformation of this fiber under tension is small until the fiber bundle breaks.

The fibers of curauá, sisal, and jute are considered high-performance fibers, as they exhibit tensile strengths above 249 MPa⁶³, a value also achieved by the aninga fiber at 308.3 MPa. This value surpasses the tensile strength of jute fiber at 249 MPa and piassava fiber at 131 MPa, with cellulose being the main component contributing to tensile strength. Also, the tensile strength of the aninga fiber places it as a fiber with strength similar to polypropylene, with a tensile strength of 386 MPa⁶⁴, and other synthetic fiber with strength in this range is polyester, as well as polyamide and polyethylene terephthalate (PET) fibers with 230 MPa⁶⁵.

Mechanical properties of the unidirectional sheet

The tested material consisted of an epoxy resin film with *Montrichardia linifera* fibers embedded in this polymeric matrix, and the following results (Fig. 7) provide the tensile strength of the sample and the modulus of elasticity.

The samples exhibited average values of 104.6 N for maximum breaking force, 4.981 MPa for breaking stress, and 332.9 MPa for modulus of elasticity.

In a study testing epoxy composite with wheat fiber, as the fiber loading increased, the strength value decreased from 6.13 MPa to 2.99 MPa, with the maximum tensile strength value found to be 7.27 MPa⁶⁶. Composites reinforced with hemp and flax fibers manufactured based on biopolymer and epoxy resin showed final tensile strengths of 5.89 MPa, demonstrating excellent mechanical properties such as tensile and flexural strength⁶⁷. The composite material with banana and coconut fiber supported tensions of up to 9.43 MPa, indicating its potential use in locations where tensile loads are applied⁵⁸.

Table 2 expresses the modulus of elasticity of the aninga composite in comparison to other thermoset composites with natural fibers.

The modulus of elasticity found falls within the range most commonly seen in composites already used with natural fibers (> 100 MPa), which indicates that the material's elastic deformation does not cause significant changes in structure until it collapses under stress when exceeding the maximum supported stress. However, the tensile strength property of the material can be improved with enhancements in the finishing of the test specimens, the addition of a greater number of fiber plies, different orientations, and better conformation with the polymeric resin, which will likely increase the value of this characteristic, given that the fiber exhibited rupture tension in the range of strength of the main natural fibers already used in composites.

The growing use of plant-based natural fibers in composite materials highlights a significant shift towards sustainability, driven by their biodegradability, eco-friendliness, and renewable nature⁶⁹. These fibers are increasingly replacing synthetic alternatives, particularly in industries like automotive and aerospace, due to

Fiber type	Tensile strength (MPa)	Elastic modulus (MPa)	Elongation (%)	Fiber diameter (μm)	Density (g/cm^3)
Aninga	308	13.000	3.9	7.50–13.25	0.19
Bambu ^{4,58}	290	1.800–6.150	-	240.00–330.00	1.15
Jute ^{25,59}	249–400	1000–3000	1.5 – 0.8	40.00–350.00	-
Coconut ^{59,60}	220	400–600	30.0	100.00–450.00	-
Curauá ^{61,62}	87–1150	800–1400	-	50.00–100.00	1.40

Table 1. Properties of *aninga* fibers and comparison with other natural fibers.

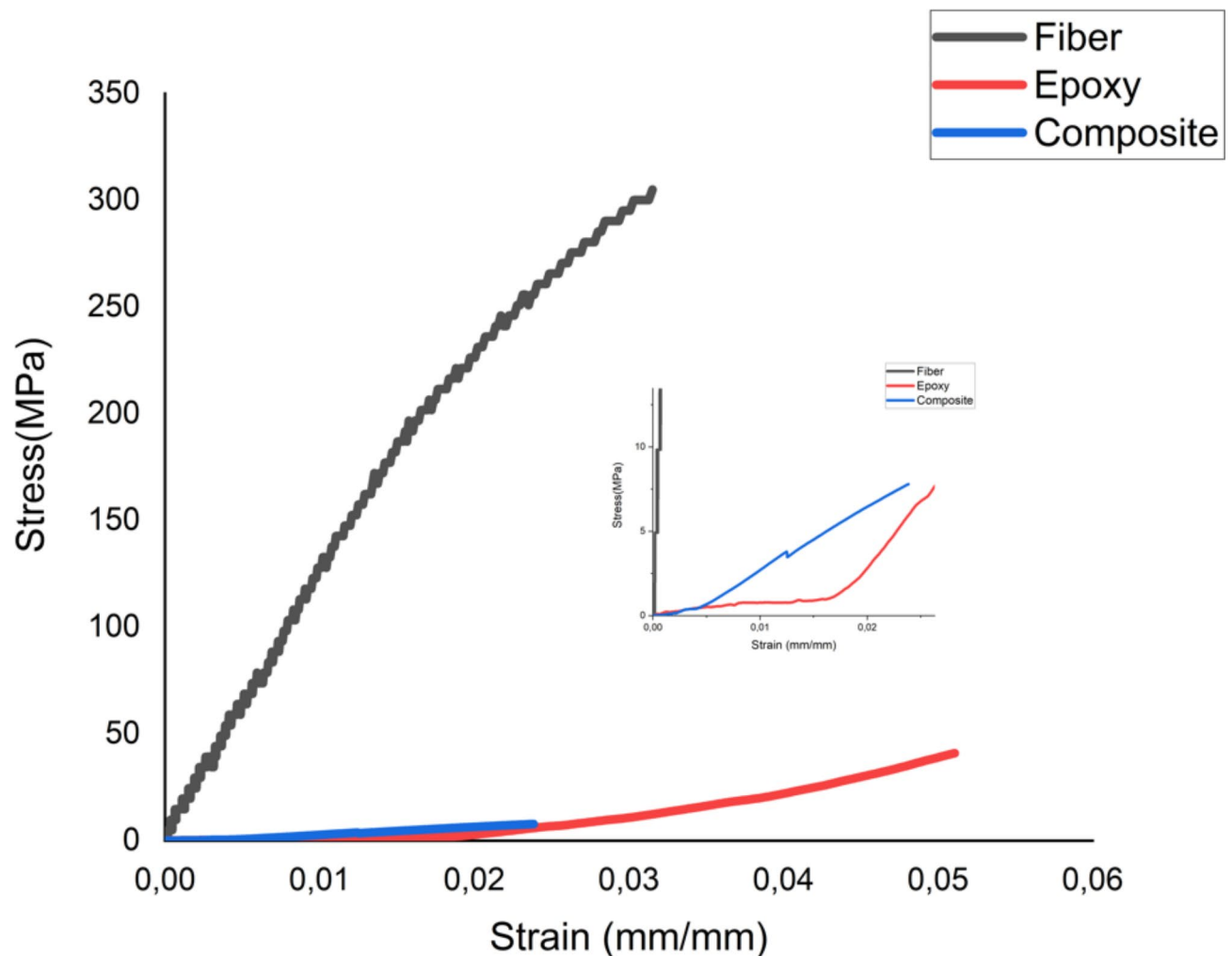


Fig. 7. Tensile strength of the single fiber, unidirectional sheet of aninga and epoxy, a single epoxy sheet and they together.

Layer	Elasticity modulus (MPa)
Neat epoxy ⁶⁸	300.0-600.0
Aninga and epoxy	332.9
Coconut, jute, coconut, and epoxy ⁶²	225.0

Table 2. Comparisons with other sheets.

their excellent physicochemical properties⁷⁰. Simultaneously, advancements in composite fabrication are crucial, emphasizing the need for new materials and processes that enhance both sustainability and efficiency⁷¹. This includes innovative treatments for natural fibers and the integration of biodegradable matrices, paving the way for the development of more durable and environmentally responsible composite materials. These findings underscore the critical importance of continuing research and development in this field to fully realize the potential of plant-based composites in various high-performance applications.

Conclusion

This research provides a comprehensive characterization of natural fibers extracted from the stem of *Montrichardia linifera* (aninga) and demonstrates their application in developing a unidirectional polymeric sheet. The study employed various analytical techniques to thoroughly investigate the properties and potential of these fibers. Fourier Transform Infrared Spectroscopy (FTIR) confirmed the presence of functional groups related to cellulose, hemicellulose, and lignin, which are essential components contributing to the fiber's structural integrity and mechanical properties. Peaks observed at 3328 cm^{-1} , 1600 cm^{-1} , and 1021 cm^{-1} highlighted the stretching vibration of the O–H bond, the carbonyl stretch in hemicellulose, and the aromatic ring vibration, respectively,

indicating the fiber's chemical composition. X-ray Diffraction (XRD) analysis revealed a crystallinity index of 62.21%, a significant indicator of the highly crystalline nature of the cellulose within the fibers. This crystallinity is crucial for mechanical strength and rigidity, which are desirable traits in materials used for reinforcement in composites. The main diffraction peak at 24.7° further emphasized the presence of crystalline cellulose, while the secondary peaks indicated the presence of amorphous materials, such as hemicellulose and lignin, which contribute to the fiber's overall mechanical behavior. Scanning Electron Microscopy (SEM) provided insights into the microstructural characteristics of the fibers. The fibers exhibited a rough surface with grooves, which are advantageous for mechanical anchoring when combined with polymeric matrices. This surface roughness, along with the honeycomb-like structure observed in the fiber bundles, enhances the bonding between the fiber and the resin, leading to improved composite performance. Additionally, Energy Dispersive Spectroscopy (EDS) analysis confirmed that carbon is the major component of the fibers, making up 70% of their composition, which aligns with the high cellulose content. Thermogravimetric Analysis (TGA) showed that the thermal stability of the fibers extends up to 450 °C, making them suitable for applications requiring high thermal resistance. The mechanical properties of the untreated fibers were also notable, with a tensile strength of 332 MPa and an elastic modulus of 13,000 MPa, classifying them as high-performance fibers suitable for reinforcing materials. The unidirectional polymeric sheet fabricated with these fibers exhibited a tensile strength of 4.5 MPa and an elasticity modulus of 332.9 MPa. Although these values are lower compared to the raw fibers, they demonstrate the potential of *Montrichardia linifera* fibers in composite material applications, particularly in the automotive industry for internal components. Furthermore, the use of *Montrichardia linifera* fibers, derived from a widespread and renewable plant species in the Amazon region, supports the development of sustainable materials. The plant's abundant availability and favorable ecological characteristics make it an ideal candidate for continuous supply in industrial applications. In conclusion, this study underscores the technological potential of *Montrichardia linifera* fibers as a sustainable and high-performance material for composite applications. The combination of favorable mechanical properties, thermal stability, and eco-friendly nature makes these fibers a promising alternative to synthetic fibers in various engineering and commercial applications. Future research could further explore the optimization of fiber-matrix bonding and the development of composites with enhanced mechanical performance.

Future scope of this study

In future studies, other fiber orientation forms may be analyzed, incorporated into various polymeric materials, and other parameters of mechanical characterization, such as impact resistance and flexural strength.

Data availability

The results presented in this article are part of a patent application in progress in Brazil (BR 10 2024 019432 2), related to the described invention. The data used and analyzed during the study are available from the corresponding author upon justified request.

Received: 20 June 2024; Accepted: 10 September 2024

Published online: 21 October 2024

References

- Hiwa, B., Ahmed, Y. M. & Rostam, S. Evaluation of tensile properties of Meriz fiber reinforced epoxy composites using Taguchi method. *Results Eng.* **18**, 101037. <https://doi.org/10.1016/j.rineng.2023.101037> (2023).
- Venkatarajan, S., Athijayamani, A. An overview on natural cellulose fiber reinforced polymer composites. *Mater. Today Proc.* **37**, 3620–3624 <https://doi.org/10.1016/j.matpr.2020.09.773> (2021).
- Prabhu, L.S. et al. A review on natural fiber reinforced hybrid composites: Chemical treatments, manufacturing methods, and potential applications. *Mater. Today Proc.* **45**(xxxx), 8080–8085. <https://doi.org/10.1016/j.matpr.2021.01.280> (2021).
- Kumar, R., Ganguly, A. & Purohit, R. A. Properties and applications of bamboo and bamboo fiber composites. *Mater. Today Proc.* <https://doi.org/10.1016/j.matpr.2023.08.162> (2023).
- Sundarababu, J., Anandan, S. S. & Griskevicius, P. Evaluation of mechanical properties of biodegradable coconut shell/rice husk powder polymer composites for lightweight applications. *Mater. Today Proc.* **39**(xxxx), 1241–1247 <https://doi.org/10.1016/j.matpr.2020.04.095> (2020).
- Lima, W. A., dos Sousa, S., de Brabo, A. C., Junior, D. R. L., Dias, C. G. & J. L., & B. T. Development and characterization of a polymeric composite from the endocarp of murumuru (*Astrocaryum Murumuru* Mart.) and recycled polyolefins. *Matéria (Rio De Janeiro)* **27**(4), e20220160. <https://doi.org/10.1590/1517-7076-RMAT-2022-0160> (2022).
- Majumder, A. et al. Jute fiber-reinforced mortars: Mechanical response and thermal performance. *J. Build. Eng.* **66**, 105888. <https://doi.org/10.1016/j.jobte.2023.105888> (2023).
- Amarante, C. B., Solano, F. A. R., Lins, A. L. F. A., Müller, A. H. & e Müller, R. C. S. *Physical, Chemical, and Nutritional Characterization of Atinga Fruit*. vol. 29, 295–303 (Planta Daninha, 2011).
- Lins, A. L. F. A. Aspectos morfológicos e anatômicos de raízes do gênero *Montrichardia* Crüger. (Araceae). Porto Alegre. 91 p. Dissertação (Mestrado em Botânica), Universidade Federal do Rio Grande do Sul (1994).
- Amaral, E. L. S., Brabo, D. R., Lopes Junior, J. L. & Amarante, C. B. Study of fibers obtained from the vegetable species *montrichardia linifera* (Araceae) to evaluation of their technological application. In *24th ABCM International Congress of Mechanical Engineering* (2017).
- Bhunia, A. K. et al. Characterization of a new natural novel lignocellulose fiber resource from the stem of *Cyperus platystylis* R.Br. *Sci. Rep.* **13**, 9699. <https://doi.org/10.1038/s41598-023-35888-w> (2023).
- Thandavamoorthy, R., Devarajan, Y. & Kaliappan, N. Antimicrobial, function, and crystalline analysis on the cellulose fiber extracted from the banana tree trunks. *Sci. Rep.* **13**, 15301. <https://doi.org/10.1038/s41598-023-42160-8> (2023).
- Heckadka, S. S. et al. Comparative evaluation of chemical treatment on the physical and mechanical properties of areca frond, banana, and flax fibers. *J. Nat. Fibres* **19** (4), 1531–1543. <https://doi.org/10.1080/15440478.2020.1784817> (2022).
- Oliveira, J. G. A. de. Microscopia Digital e Análise de Imagens para Caracterização de Tubos Compósitos Fabricados por Enrolamento Filamentar, 82 (2008).

15. ASTM D3039/D3039M-00. *Standard Test Method for Tensile Properties of Polymer Matrix Composite Materials* (ASTM International, 2000).
16. Elamin, M. A. M. et al. Preparation and characterization of wood-plastic composite by utilizing a hybrid compatibilizer system. *Ind. Crops Prod.* **154**(January), 112659 (2020).
17. Tamanna, T. A., Belal, S. A., Shibly, M. A. H. & Khan, A. N. Characterization of a new natural fiber extracted from *Corypha taliera* fruit. *Sci. Rep.* **11**(1), 7622. <https://doi.org/10.1038/s41598-021-87128-8> (2021).
18. Basak, S. et al. Development of natural fiber-based flexural composite: A sustainable mimic of natural leather. *Mater. Today Commun.* **32**, 2352–4928. <https://doi.org/10.1016/j.mtcomm.2022.103976> (2022).
19. Tiwari, Y. M., Sarangi, S. K. & Part, B. Characterization of raw and alkali treated cellulosic *Grewia Flavescens* natural fiber. *Int. J. Bio. Macromol.* **209**, 1933–1942. <https://doi.org/10.1016/j.ijbiomac.2022.04.169> (2022).
20. Shahril, S. M. et al. Alkali treatment influence on cellulosic fiber from *Furcraea foetida* leaves as potential reinforcement of polymeric composites. *J. Mater. Res. Technol.* **19**, 2567–2583. <https://doi.org/10.1016/j.jmrt.2022.06.002> (2022).
21. Manimaran, P. et al. Characterization of new cellulosic fiber: *Dracaena reflexa* as a reinforcement for polymer composite structures. *J. Mater. Res. Technol.* (2019).
22. Bhunia, A. K., Mondal, D., Sahu, K. R. & Mondal, A. K. Characterization of new natural cellulosic fibers from *Cyperus compactus* Retz. (Cyperaceae) Plant. *Carbohydr. Polym. Technol. Appl.* **5**, 100286. <https://doi.org/10.1016/j.carpta.2023.100286> (2023).
23. Manimaran, P. et al. A. M. Extraction and characterization of natural lignocellulosic fibers from *Typha angustata* grass. *Int. J. Bio. Macromol.* **222**(Part B), 1840–1851 (2022).
24. Hou, G., Zhao, S., Fang, P. L. & Isogai, Z. A systematic study for the structures and properties of phosphorylated pulp fibers prepared under various conditions. *Cell.* <https://doi.org/10.1007/s10570-022-04713-4> (2022).
25. Vijay, R. et al. Characterization of novel natural fiber from *Saccharum bengalense* grass (Sarkanda). *J. Nat. Fibers* **17** (12), 1739–1747. <https://doi.org/10.1080/15440478.2019.1598914> (2020).
26. Miranda, C. S., Fiuza, R. P., Carvalho, R. F. & José, N. M. Efeito dos tratamentos Superficiais Nas propriedades do bagaço da fibra de piaçava *Attalea funifera martius*. *Quim. Nova* **38**, 161–165 (2015).
27. Zhang, Y. et al. Cellulose nanofibril-reinforced biodegradable polymer composites obtained via a Pickering emulsion approach. *Cellulose* **24**, 3313–3322 (2017).
28. Gao, C. et al. Quantitative and qualitative characterization of dual scale mechanical enhancement on cellulosic and crystalline-structural variation of NaOH treated wheat straw. *Bioresour. Technol.* **312**, 123535 (2020).
29. Hafid, H. S. et al. Enhanced crystallinity and thermal properties of cellulose from rice husk using acid hydrolysis treatment. *Carbohydr. Polym.* **260**, 117789 (2021).
30. Sankhla, S., Hossain, S. H. & Neogi, S. Greener extraction of highly crystalline and thermally stable cellulose micro-fibers from sugarcane bagasse for cellulose nano-fibrils preparation. *Carbohydr. Polym.* **251**, 117030. <https://doi.org/10.1016/j.carbpol.2020.117030> (2021).
31. Mo, R. J., Zhao, Y., Zhao, M. M., Wu, M. & Wang, C. Graphene-like porous carbon from sheet cellulose as electrodes for supercapacitors. *Chem. Eng. J.* **346**, 104–112. <https://doi.org/10.1016/j.cej.2018.04.010> (2018).
32. Balaji, A. N., Karthikeyan, M. K. V. & Vignesh, V. Characterization of new natural cellulosic fiber from kusha grass. *Int. J. Polym. Anal. Charact.* **21**, 599–605. <https://doi.org/10.1080/1023666X.2016.1192324> (2016).
33. Sreenivasan, V. S., Somasundaram, S., Manikandan, R. D. & Narayanasamy, V. Microstructural, physicochemical and mechanical characterization of *Sansevieria cylindrica* fibers – an exploratory investigation. *Mater. Des.* **32**, 453–461. <https://doi.org/10.1016/j.matdes.2010.06.004> (2011).
34. Sathishkumar, T. P., Navaneethakrishnan, P., Shankar, S. & Rajasekar, R. Characterization of new cellulose *Sansevieria ehrenbergii* fibres for polymer composites. *Compos. Interfaces* **20**, 575–593. <https://doi.org/10.1080/15685543.2013.816652> (2013).
35. Suryanto, H., Marsyahyo, E., Irawan, Y. S. & Soenoko, R. Morphology, structure, and mechanical properties of natural cellulose fiber from mendong grass (*Fimbristylis globulosa*). *J. Nat. Fibers* **11**, 333–351. <https://doi.org/10.1080/15440478.2013.879087> (2014).
36. Sanjay, M. R., Siengchin, S., Parameswaranpillai, J., Jawaid, M. & Ozbakkaloglu, T. Lignocellulosic fiber reinforced composites: Progress, performance, properties, applications, and future perspectives. *Polym. Compos.* **43**, 645–691. <https://doi.org/10.1002/pc.26413> (2022).
37. Vijay, R., Vinod, A., Singaravelu, D. L., Sanjay, M. R. & Siengchin, S. Characterization of chemically treated and untreated natural fibers from *Pennisetum orientale* grass- a potential reinforcement for lightweight polymeric applications. *Int. J. Light Mater. Manuf.* **4**, 43–49. <https://doi.org/10.1016/j.ijlmm.2020.06.008> (2021).
38. Corrente, G. A. et al. Chemical–physical and dynamical–mechanical characterization on *Spartium junceum* L. cellulosic fiber treated with softener agents: A preliminary investigation. *Sci. Rep.* **11**, 35. <https://doi.org/10.1038/s41598-020-79568-5> (2021).
39. Maache, M., Bezazi, A., Amroune, S., Scarpa, F. & Dufresne, A. Characterization of a novel natural cellulosic fiber from *Juncus effusus* L. *Carbohydr. Polym.* **171**, 163–172. <https://doi.org/10.1016/j.carbpol.2017.04.096> (2017).
40. Moshi, A. M. A. et al. Characterization of natural cellulosic fiber extracted from *Grewia damine* flowering plant's stem. *Int. J. Biol. Macromol.* **164**, 1246–1255. <https://doi.org/10.1016/j.ijbiomac.2020.07.225> (2020).
41. Ding, L. et al. Characterization of natural fiber from *manau rattan* (Calamus Manan) as a potential reinforcement for polymer-based composites. *J. Bioresour. Bioprod.* **7**(3), 190–200. <https://doi.org/10.1016/j.jobab.2021.11.002> (2022).
42. Hossain, S., Jalil, M. A., Islam, T., Rahman, M. M. A. & Low-density cellulose rich new natural fiber extracted from the bark of jack tree branches and its characterizations. *SSRN Electron. J.* **8**(November). <https://doi.org/10.2139/ssrn.4186469> (2022).
43. Srisuk, R., Techawinyutham, L., Vinod, A., Rangappa, S. M. & Siengchin, S. Agro-waste from *Bambusa flexuosa* stem fibers: A sustainable and green material for lightweight polymer composites. *J. Build. Eng.* **73**, 2352–7102. <https://doi.org/10.1016/j.jobe.2023.106674> (2023).
44. Indran, S. & Raj, R. E. Characterization of new natural cellulosic fiber from *Cissus quadrangularis* stem. *Carbohydr. Polym.* **117**, 392–399. <https://doi.org/10.1016/j.carbpol.2014.09.072> (2015).
45. Chakravarthy, S. K., Madhu, S., Raju, J. S. N. & Shariff, J. M. D. Characterization of novel natural cellulosic fiber extracted from the stem of *Cissus Vitiginea* plant. *Int. J. Biol. Macromol.* **161**, 1358–1370. <https://doi.org/10.1016/j.ijbiomac.2020.07.230> (2020).
46. Manimaran, P., Senthamaraikannan, P., Sanjay, M. R., Marichelvam, M. K. & Jawaid, M. Study on the characterization of *Furcraea foetida* new natural fiber as composite reinforcement for lightweight applications. *Carbohydr. Polym.* **181**, 650–658. <https://doi.org/10.1016/j.carbpol.2017.11.099> (2018).
47. Majhi, S., Pradhan, S., Prakash, V. & Acharya, S. K. Influence of fiber surface modification on impact strength behavior of *Agave Lechuguilla* fiber reinforced polymer composites. *Mater. Today Proc.* <https://doi.org/10.1016/j.matpr.2023.02.416> (2023).
48. Kumar, N. P., Chellapandian, M., Arunachalam, N. & Vincent, P. Effect of mercerization on the chemical characteristics of plant-based natural fibers. *Mater. Today Proc.*, **68**(Part 5), 1201–1207. <https://doi.org/10.1016/j.matpr.2022.05.319> (2022).
49. Balasubramanian, B., Raja, K., Vignesh Kumar, V. & Ganeshan, P. Characterization study of *Holoptelea Integrijolia* tree bark fibers reinforced epoxy composites. *Nat. Prod. Res.* **1**, 1–10. <https://doi.org/10.1080/14786419.2022.2137505> (2022).
50. Lazzari, L. K., Neves, R. M., Vanzetto, A. B., Zattera, A. J. & Santana, R. M. C. Thermal degradation kinetics and lifetime prediction of cellulose biomass cryogels reinforced by its pyrolysis waste. *Mater. Res.* **25**, e20210455. <https://doi.org/10.1590/1980-5373-MR-2021-0455> (2022).
51. Thomason, J. L. & Rudeiros-Fernández, J. L. Thermal degradation behavior of natural fibers at thermoplastic composite processing temperatures. *Polym. Degrad. Stab.* **188**, 109594. <https://doi.org/10.1016/j.polymdegradstab.2021.109594> (2021).

52. Kumar, R., Gunjal, J. & Chauhan, S. Effect of carbonization temperature on properties of natural fiber and charcoal filled hybrid polymer composite. *Compos. B Eng.* **217**, 108846. <https://doi.org/10.1016/j.compositesb.2021.108846> (2021).
53. Mudoji, M. P. & Sinha, S. Thermal degradation study of natural fiber through thermogravimetric analysis. *Mater. Today Proc.* <https://doi.org/10.1016/j.matpr.2023.05.362> (2023).
54. Saravanakumar, S. S., Kumaravel, A., Nagarajan, T., Sudhakar, P. & Baskaran, R. Characterization of a novel natural cellulosic fiber from *Prosopis juliflora* bark. *Carbohydr. Polym.* **92**, 1928–1933 (2013).
55. Liu, Q. et al. Isolation of high-purity cellulose nanofibers from Wheat Straw through the combined environmentally friendly methods of steam explosion, microwave-assisted hydrolysis, and microfluidization. *ACS Sustain. Chem. Eng.* **5**(7), 6183–6191. <https://doi.org/10.1021/acssuschemeng.7b01108> (2017).
56. Azanaw, A., Haile, A. & Gideon, R. K. Extraction and characterization of fibers from *Yucca Elephantine* plant. *Cellulose* **26**, 795–804. <https://doi.org/10.1007/s10570-018-2103-x> (2019).
57. Seki, Y., Sarikanat, M., Sever, K. & Durmuşkahya, C. Extraction and properties of *Ferula communis* (chakshir) fibers as novel reinforcement for composites materials. *Compos. B Eng.* **44**(1), 517–523 (2013).
58. Gayathri, N., Joyson, S. V. K., Aakash, A. & Joseph, M. A. G. Mechanical properties investigation on natural fiber reinforced epoxy polymer composite. *Mater. Today Proc.* **72**(Part 4), 2574–2580. <https://doi.org/10.1016/j.matpr.2022.10.121> (2023).
59. Gurajala, N. K., Sanjeev, L., Teja, B., Kumar, T. S. & Manikanta, J. E. An overview of mechanical properties of biodegradable polymers and natural fiber materials. *Mater. Today Proc.* <https://doi.org/10.1016/j.matpr.2023.05.161> (2023).
60. Mohammed, J. K. et al. Comprehensive insights on mechanical attributes of natural-synthetic fibers in polymer composites. *J. Mater. Res. Technol.* **25**, 4960–4988. <https://doi.org/10.1016/j.jmrt.2023.06.148> (2023).
61. Velmurugan, V., Kumar, D. D., Thanikaikarasan, S. Experimental evaluation of mechanical properties of natural fiber reinforced polymer composites. *Mater. Today Proc.* <https://doi.org/10.1016/j.matpr.2020.05.19> (2020).
62. Yusoff, R. B., Takagi, H. & Nakagaito, A. N. A comparative study of polylactic acid (PLA)-based unidirectional green hybrid composites reinforced with natural fibers such as kenaf, bamboo, and coir. *Hybrid. Adv.* **3**, 100073. <https://doi.org/10.1016/j.hybadv.2023.100073> (2023).
63. Fidelis, M. E. A., Pereira, T. V. C., Gomes, O., Silva, F. M. & Filho, F. D. E. A. da R. D. T. The effect of fiber morphology on the tensile strength of natural fibers. *J. Mater. Res. Technol.* **2**(2), 149–157. <https://doi.org/10.1016/j.jmrt.2013.02.003> (2013).
64. Zhang, Z. et al. Simultaneously enhanced interfacial shear strength and tensile strength of heterocyclic aramid fiber by graphene oxide. *Nano Res.* **16**, 12286–12293. <https://doi.org/10.1007/s12274-023-5904-7> (2023).
65. Tomisawa, R. et al. Tensile strength of polyester fiber estimated by molecular-chain extension prior to structure formation. *Sci. Rep.* **13**, 11759. <https://doi.org/10.1038/s41598-023-38987-w> (2023).
66. Sharma, P., Pradhan, S., Sharma, Y. K., Dangayach, G. S. & Patnaik, A. Experimental investigation on physical and mechanical properties of wheat fiber filled epoxy composites. *Mater. Today Proc.* <https://doi.org/10.1016/j.matpr.2023.03.823> (2023).
67. Ahmed, J. P. S., Sudarsan, S., Parthiban, E., Trofimov, E. & Sridhar, B. Exploration of mechanical properties of hemp fiber/flax fiber reinforced composites based on biopolymer and epoxy resin. *Mater. Today Proc.* <https://doi.org/10.1016/j.matpr.2023.03.790> (2023).
68. Elfaleh, I. et al. A comprehensive review of natural fibers and their composites: An eco-friendly alternative to conventional materials. *Results Eng.* **19**, 101271. <https://doi.org/10.1016/j.rineng.2023.101271> (2023).
69. Syduzzaman, M., Faruque, M. A. A., Bilisik, K. & Naebe, M. Plant-based natural fibre reinforced composites: A review on fabrication, properties and applications. *Coatings* **10**(10), 973. <https://doi.org/10.3390/coatings10100973> (2023).
70. Marques, M. D. V., Melo, R. P., Araujo, R. D., Lunz, J. D. & Aguiar, V. D. *Recent Trends in Surface Modification of Natural Fibres for Their Use in Green Composites* (SpringerLink, 2023). <https://doi.org/10.1007/s11665-023-07491-1>
71. Aydin, M., Tozlu, H. & Kemaloglu, S. A review of natural fiber composites: Properties, modification and processing techniques, characterization, applications. *J. Mater. Sci.* **58**, 527–564. <https://doi.org/10.1007/s10853-023-07730-1> (2023).

Author contributions

J. L. L. J. – The author produced this article, obtaining the main information and writing this article; D. R. B. – This author made the fiber extraction from aninga plant and helped in the tensile strength analysis; E. L. S. A. – This author made the fiber extraction and made the SEM analysis; (A) W. da C. R. – This author made the graphics of FTIR and XDR and the interpretation of data; C. (B) do (A) – This author helped with the writing manuscript and supervised the experiments; C. G. (B) T. D. – This author leads this article, in the conception and supervision of the mechanical analysis of fiber.

Declarations

Competing interests

The authors declare no competing interests.

Additional information

Supplementary Information The online version contains supplementary material available at <https://doi.org/10.1038/s41598-024-72781-6>.

Correspondence and requests for materials should be addressed to J.L.L.J.

Reprints and permissions information is available at www.nature.com/reprints.

Publisher's note Springer Nature remains neutral with regard to jurisdictional claims in published maps and institutional affiliations.

Open Access This article is licensed under a Creative Commons Attribution-NonCommercial-NoDerivatives 4.0 International License, which permits any non-commercial use, sharing, distribution and reproduction in any medium or format, as long as you give appropriate credit to the original author(s) and the source, provide a link to the Creative Commons licence, and indicate if you modified the licensed material. You do not have permission under this licence to share adapted material derived from this article or parts of it. The images or other third party material in this article are included in the article's Creative Commons licence, unless indicated otherwise in a credit line to the material. If material is not included in the article's Creative Commons licence and your intended use is not permitted by statutory regulation or exceeds the permitted use, you will need to obtain permission directly from the copyright holder. To view a copy of this licence, visit <http://creativecommons.org/licenses/by-nc-nd/4.0/>.

© The Author(s) 2024